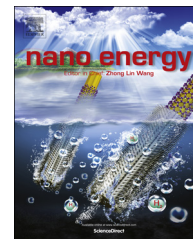


Available online at [www.sciencedirect.com](http://www.sciencedirect.com)

ScienceDirect

journal homepage: [www.elsevier.com/locate/nanoenergy](http://www.elsevier.com/locate/nanoenergy)

## COMMUNICATION

# Nano-porous sulfur-polyaniline electrodes for lithium-sulfurbatteries



Jianhua Yan<sup>a,b</sup>, Bingyun Li<sup>b</sup>, Xingbo Liu<sup>a,\*</sup>

<sup>a</sup>Department of Mechanical and Aerospace Engineering, West Virginia University, Morgantown, WV 26506, USA

<sup>b</sup>Biomaterials, Bioengineering & Nanotechnology Laboratory, West Virginia University, Morgantown, WV 26506, USA

Received 2 September 2015; received in revised form 17 October 2015; accepted 28 October 2015  
Available online 5 November 2015

**KEYWORDS**

Li-S battery;  
Polyaniline;  
Sulfurized carbon;  
Nanoporous;  
Energy storage

**Abstract**

Here we report a nano-porous sulfur-polyaniline (SPANI) electrode with high sulfur loading, excellent cycling and rate capability for Li-S batteries. The SPANI has a high degree of interconnected nano-porous structures conducive to large sulfur loading and fast mass transportation. In addition, a disulfide chain on PANI is also functioned as the electrochemical redox component. While the main positively charged backbone chain in SPANI provides electron conductivity and electrostatic attraction force to stabilize polysulfide anions during cycling. As a result, the SPANI electrode demonstrates a high reversible capacity of  $750 \text{ mA h g}^{-1}$  with 89.7% of capacity retention over 200 cycles at 0.3 C, and an excellent high-rate response up to 2 C over 200 cycles with a good sulfur utilization. The covalently bonded sulfur on positively charged polymer substrate offers a new way to improve energy storage capabilities of Li-S batteries.

© 2015 Elsevier Ltd. All rights reserved.

**Introduction**

Rechargeable batteries played an important role in many applications, ranging from the wearable devices to large-scale stationary electrical energy storage. Lithium-ion and sodium-ion batteries have been widely studied as renewable

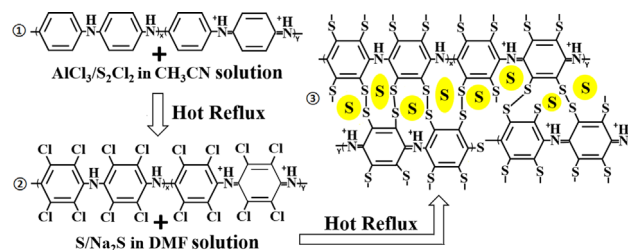
energy for these applications [1,2]. However, these batteries with insertion cathode materials have limited their specific energy to  $200\text{--}300 \text{ W h kg}^{-1}$ , unable to meet the ever-growing energy demands. The development of new rechargeable battery systems could solve the problem and fuel the various energy applications. As a candidate, Li-S battery that adopts integrated chemistry has attracted great interest in recent years due to their high theoretical energy density ( $2600 \text{ W h kg}^{-1}$ ) [3]. In addition, Li-S battery has been proposed to be an inexpensive alternative of

\*Corresponding author. Tel.: +1 304 293 3339; fax: +1 304 293 7070.  
E-mail address: [xingbo.liu@mail.wvu.edu](mailto:xingbo.liu@mail.wvu.edu) (X. Liu).

current batteries, owing to the low cost of sulfur, and thus may leveling the cost-efficient nature of renewable energy. However, the commercialization of Li-S batteries is still challenged by insufficient cycle life with a rapid capacity fade, mainly originating from the nonconductive sulfur and polysulfide species dissolution into liquid electrolyte [4]. Despite two decades of intensive efforts and advancements achieved in fundamental electrochemistry and performance improvements, the dissolution and migration of polysulfide species and their side reactions with the lithium anode are still an open problem [5].

Most researchers focused on the fabrication of various sulfur carbon composites or smart sulfur electrode structures to reduce the dissolution of polysulfide species from cathodes into the liquid electrolyte by providing physical adsorption forces [6-13]. However, physical barriers can only slow down the sulfur dissolution in the short term because the migration of soluble polysulfide species is caused by the electrical field in the cells [14,15]. With this in mind, researchers developed a new type of cathode based on sulfurized-carbon (SC), which chemically bonds sulfur onto the carbon host [15] and thus inhibits the dissolution of polysulfide species. Conductive materials such as polyacrylonitrile (PAN) and carbon nanotubes (CNT) have been found suitable in the fabrication of SC materials due to their special surface functional groups (i.e.  $C \equiv N$  in PAN and  $C=C$  in CNT) [14,16-18]. However, most of these SC materials fabricated with the traditional strategy had low sulfur content and insufficient cycle life when used in sulfur electrode. Reaction of carbon with sulfur at a high temperature was the most common method to fabricate SC materials, which resulted in a low sulfur content because of the evaporation of sulfur. In addition, the chemical bonded sulfur greatly decreased the conductivity of host carbon. These two issues neutralized the advantages of Li-S batteries. Therefore, better sulfurization technology should be developed.

Here, we report a facile chemical approach to fabricate nanoporous sulfur-polyaniline (SPANI) that affords high sulfur content (65 wt%) and electric/ionic conductivity. The SPANI contains three parts: a main backbone chain providing electron conductivity; a high degree of interconnected nano-porous structures conducive to large elemental sulfur loading and fast ionic conduction and mass transportation; and a disulfide side chain functioning as the second electrochemical redox component. PANI is well known as a conductive and electroactive polymer, which also provides strong affinity and high loading of sulfur and polysulfides [19-25]. In addition, the multiple positively charged amino-containing surface groups on its backbones also favor catenating and stabilizing polysulfide anions during cycling [22]. Therefore the electrical contact between sulfur and PANI during cycling can be guaranteed by the strong chemical and physical confinement in this nanoporous SPANI structures. As a result, the Li-S batteries employing SPANI cathodes showed high efficiency of sulfur encapsulation, excellent cycling stabilities and rate capabilities. Stable reversible capacities over  $700 \text{ mA h g}^{-1}$  at 0.3 C,  $600 \text{ mA h g}^{-1}$  at 0.6 C, and  $500 \text{ mA h g}^{-1}$  at 1 C over 200 cycles were obtained. The capacity is calculated based on sulfur weight.



Scheme 1 Synthesis routes of SPANI.

## Materials and methods

### Preparation of SPANI cathodes

In present study, SPANI was fabricated with a wet chemical method, which involved *in-situ* chlorinated substitution and vulcanization reactions. The detailed synthesis procedures were summarized in the supplemental information, and shown in Scheme 1. Briefly, the polychloride groups were first created *in situ* by chlorination of the pristine PANI nanoparticles. These polychloride groups were then substituted by polysulfide groups through *in situ* vulcanization reaction. After the two-step reaction, the SPANI composites were extracted from acetone solution. Last, the SPANI was annealed at  $159^\circ\text{C}$  in a vacuum oven for 5 h to further anchor sulfur onto the SPANI surfaces. Sulfur content in SPANI was 65 wt%, which contained elemental sulfur and disulfide bonds on SPANI chains. Cathode slurries contained 80 wt% of SPANI, 10 wt% of carbon black, and 10 wt% of polyvinylidene fluoride (PVDF). Sulfur loading in the cathode was  $\sim 3.01 \text{ mg cm}^{-2}$ .

### Physical characterization

Scanning electron microscopy (SEM) characterizations were performed with a working distance of 12 cm. All the samples were attached to conductive copper tape directly for imaging. Energy dispersive X-ray spectrometry (EDS) was performed with the connection of SEM device. Crystal structure characterization was conducted with a PANalytical X-ray diffraction (XRD) with  $\text{Cu K}\alpha$  radiation between  $10^\circ$  and  $60^\circ$  at a scan rate of  $0.1^\circ\text{s}^{-1}$ . FTS 7000 Fourier transform-infrared spectroscopy (FTIR) and Kratos Axis Ultra X-ray photoelectron spectroscopy (XPS, Kratos Analytical) with a monochromatized  $\text{Al K}\alpha$  X-ray source were used to analyze the surface chemistry of SPANI cathodes. Deconvolution of the XPS spectra was performed with a Casa XPS program with Gaussian-Lorentzian functions.

### Electrochemical measurements

CR2032-type coin cells were used for battery assembling. Lithium foils were used as the anodes, Cellgard 2400 microporous membranes as separators,  $1.0 \text{ mol L}^{-1}$  bis(tri-fluoromethane sulfonyl) imide ( $\text{LiTFSI}$ ) dissolved in dioxolane (DOL) and 1,2-dimethoxyethane (DME) (1:1, v/v) as electrolytes. The cathode material was on a  $0.8 \times 0.8 \text{ cm}^2$  square aluminum substrate, and the amount of electrolyte for each cell was  $\sim 20 \mu\text{l}$ . The cells were assembled in an argon-filled glove box. Electrochemical measurements were

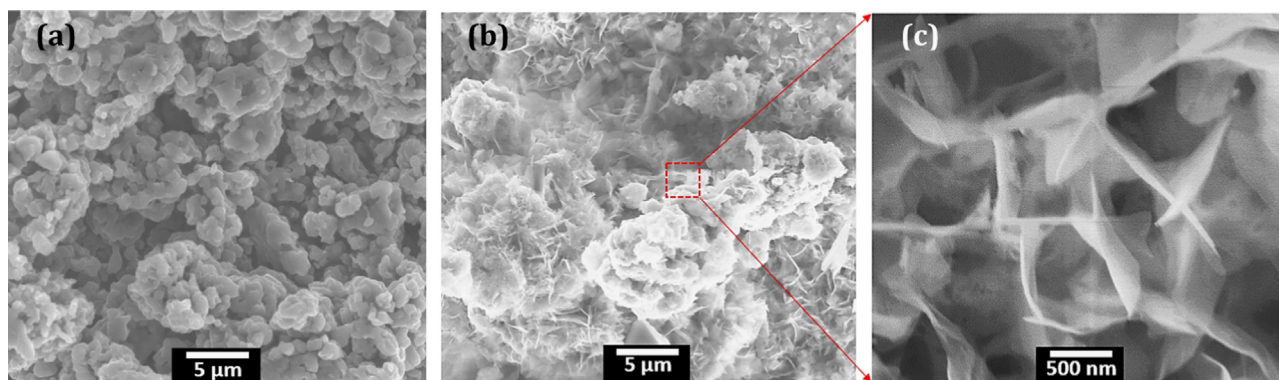


**Figure 1** SEM characterization of PANI and SPANI. (a) PANI nanoparticles, (b) synthesized coralloid SPANI composites, and (c) the nano-flakes in the coralloid SPANI granules.

performed galvanostatically between 1.0 and 3.0 V at various current densities. Capacity was calculated based on the weight of sulfur on the cathodes. The cyclic voltammograms (CV) experiments were conducted using a NOVA potentiostat at a scan rate of  $0.1 \text{ mV s}^{-1}$ . EIS measurements were carried out using a NOVA electrochemical workstation in a frequency range between 100 kHz and 100 mHz at a potentiostatic signal amplitude of 5 mV. All experiments were conducted at room temperature.

## Results

### Material characterizations

The pristine PANI had a nanoparticle morphology with an average particle size of  $1 \mu\text{m}$ , as shown in Figure 1a. Interestingly, the obtained SPANI had a hierarchical coralloid-like structure with sulfur uniformly covered on the external surface (Figure 1b). A high magnification image (Figure 1c) clearly showed that the coralloid-like structure was constructed by multiple nano-flakes, which had a high degree of interconnectivity and formed a three dimensional porous framework with increased surface areas and macro-pore volumes. As can be seen, the pore size was  $\sim 500 \text{ nm}$ . These multiple pores enhanced mass transportation because of the decreased diffusion length for the intercalating electrolyte anions, and thus facilitated more rapid battery operation. In addition, these pores could greatly alleviate the volume changes of active sulfur materials during the repeated discharging and charging processes. The formation of the hierarchical coralloid nano-flaked SPANI structure was probably due to the variation of surface energy of PANI polymers caused by the unsaturated surface functional groups in the PANI backbones during the synthesis process. The EDS and nuclear magnetic resonance (NMR) characterizations of SPANI are shown in Figures S1 and S2, which demonstrated a structural change of PANI after being reacted with sulfur, probably was caused by the substitution of hydrogen atoms with sulfur atoms in PANI backbones. In addition, the EDS analysis revealed that the sulfur content was 63 wt%.

The sulfur/disulfide bonds and sulfur content in SPANI were determined by differential scanning calorimetry (DSC) and thermogravimetric analysis (TGA), as shown in Figure 2a. Two obvious peaks were observed at 220 and  $400 \text{ }^\circ\text{C}$  in the DSC

curve of SPANI, indicating the existence of two different kinds of sulfur bonds. The one at  $220 \text{ }^\circ\text{C}$  corresponded to the decomposition of S-S bonds, and the other one belonged to the breakdown of C-S bonds on the SPANI backbones. Generally, the S-S bond has a much lower bond energy than the C-S bond (i.e.,  $418 \text{ kJ mol}^{-1}$  for the S-S bond and  $740 \text{ kJ mol}^{-1}$  for the C-S bond at room temperature) [26]. Since there was an obvious weight loss begin from  $420 \text{ }^\circ\text{C}$  in PANI curve, which may be due to the carbonization of PANI, we measured the weight loss of SPANI by reducing the weight loss of PANI at  $420 \text{ }^\circ\text{C}$ . From the weight loss analysis of TGA tests, sulfur content in SPANI was 65 wt%.

The SPANI was further characterized using XRD (Figure 2b). For PANI, the crystalline peaks appeared at  $2\theta=15.3^\circ$ ,  $20.7^\circ$ , and  $25.2^\circ$ , corresponding to the (011), (020), and (200) crystal planes of PANI in its emeraldine salt form, respectively [27]. For sulfur, all the strong diffraction peaks can be attributed to orthorhombic sulfur with high crystallinity. Clearly, the SPANI showed the characteristic peaks of both sulfur and PANI.

The structure of SPANI was determined by FTIR, as shown in Figure 2c. PANI showed characteristic bands at 3419, 1565, 1492, 1325, and  $1139 (808) \text{ cm}^{-1}$ , corresponding to the N-H, C=N, C=C, C-N, and in-plane C-H (out-of-plane C-H) stretching vibrations, respectively [28]. These results further confirmed that PANI existed in the form of emeraldine salt. In the SPANI spectra, the C-H stretching vibration at  $1109 \text{ cm}^{-1}$  could be assigned to benzenoid rings that shifted to lower wave numbers and the intensity of both C-H vibrational bands at 1109 and  $808 \text{ cm}^{-1}$  significantly weakened, indicating the replacement of H atoms on aromatic rings by S atoms. In addition, according to Yu et al. the two peaks at 915 and  $816 \text{ cm}^{-1}$  could be assigned to the vibrations of S-S bonds, the two peaks at 720 and  $529 \text{ cm}^{-1}$  could be assigned to the vibrations of C-S bonds [29].

The sulfur bonds in SPANI were further investigated using XPS, and the wide range spectra are shown in Figure 2d. Figure 2e shows the S2p spectra of the SPANI. The binding energy of the S 2p<sub>3/2</sub> peak was 163.7 eV, which is slightly lower than that of elemental sulfur at 164.0 eV, revealing the possible presence of C-S bonds. While the peak at 165.4 eV in the S 2p<sub>1/2</sub> spectra suggested that S atoms were linked to a benzenoid ring and a quinoid ring. The reason for the large peak distance of 1.4 eV could be attributed to the presence of C-S bonds and disulfide bonds in SPANI

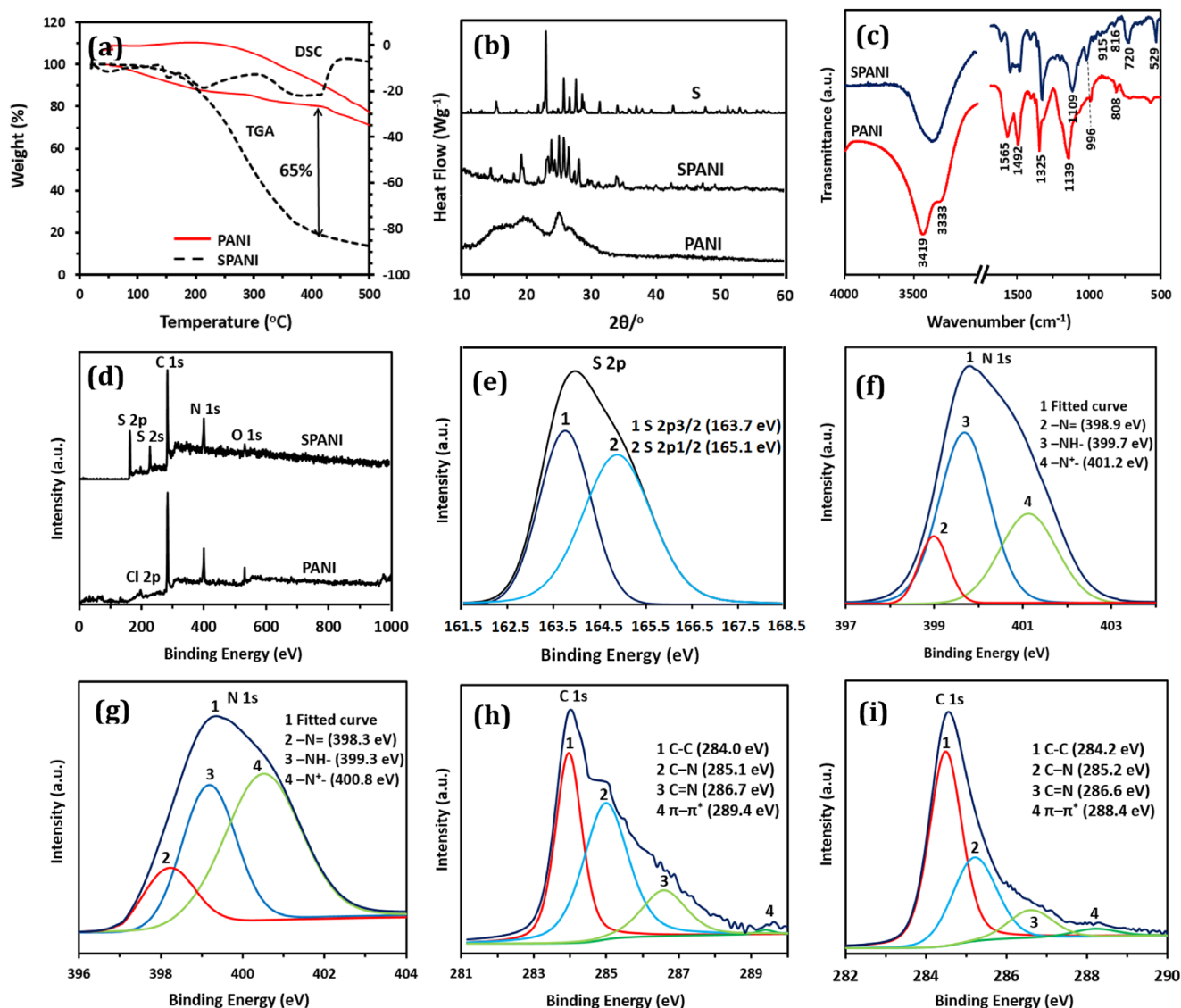


**Figure 2** Structure characterization of SPANI. (a) TGA and DSC analysis of SPANI showing 65 wt% of sulfur in SPANI composite. (b) XRD patterns of sulfur, SPANI, and PANI. (c) FTIR spectra of PANI and SPANI. (d) Wide range XPS spectra of PANI and SPANI. (e) XPS data of S 2p regions of SPANI. XPS data of C 1s regions of (f) PANI and (g) SPANI. XPS data of N 1s regions of (h) PANI and (i) SPANI.

structure. Figure 2f and 2g shows the XPS spectra of the N 1s core level of PANI and SPANI, respectively. Both of them were composed of three subpeaks, corresponding to -N=, -NH-, and -N<sup>+</sup> [30]. Compared with PANI, all the three peaks of SPANI had lower binding energies, indicating substitution of the H atom by sulfur. In addition, the ratio of [-N=]/[-NH-] for SPANI was obviously higher than that of pure PANI, further confirming the existence of chemically bonded sulfur on the SPANI backbones. Figure 2h and 2i shows the C 1s spectra of PANI and SPANI, respectively. Both of them could be separated into four fitted peaks, corresponding to C-C, C-N, C=N, and π-π\* [31,32]. Compared to PANI, the C-C and C-N peaks of SPANI shifted to higher binding energies. The tip-shift of these two peaks, due to the polar character of the C-S bonds, was evidence of the incorporation of sulfur into the PANI backbone structure. A contribution at about 288.4 eV (π-π\*), which was smaller than that in PANI, indicated that SPANI was more stable than PANI.

Based on the data from TGA, XRD, FTIR, and XPS, we believed during the wet chemical synthesis process, part of sulfur reacted with PANI to form a cross-linked porous framework with both intra- and inter-chain disulfide bonds. The rest of sulfur covered onto the surfaces or infused into the voids and nanopores of SPANI polymers. Therefore, sulfur was both physically and chemically confined in the coralloid SPANI structure. The porous SPANI framework could work not only as an additional host for Li-ion insertion/extraction, but also as a container for electrolyte to penetrate into the aggregated bulk sulfur.

## Electrochemical performance

The first five cycles' CV curve of the Li-SPANI battery at a scan rate of 0.1 mV s<sup>-1</sup> is shown in Figure 3a. We observed two cathodic peaks at ~2.25 and ~1.95 V, and two almost

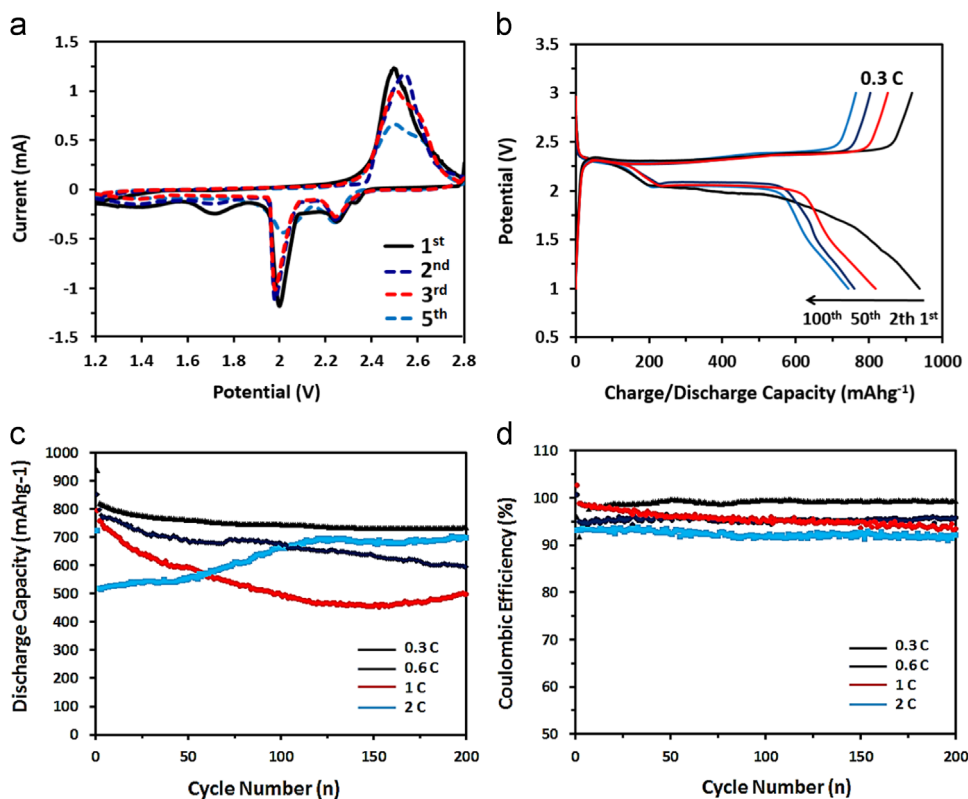


**Figure 3** Electrochemical performance of Li-S batteries employing SPANI cathodes. (a) Continuous CV curves of the battery (scanning rate was  $0.1 \text{ mV s}^{-1}$ ). (b) Cycling ability of the battery at a current rate of 0.3 C. (c) Long-term cycling stability and (d) Coulombic efficiency of the battery at different current rates.

overlapped anodic peaks at  $\sim 2.45$  and  $\sim 2.50$  V. The sulfur chemical bonds in SPANI changed the equilibrium potential of S-Li reactions, which led to a discharge potential shifting to a lower plateau. The cathodic peak at 1.70 V disappeared after the initial cycle, probably due to the rearrangement of the active sulfur materials to electrochemically favorable positions after their dissolution into the liquid electrolyte during the first cycles. The CV curves in the subsequent cycles showed good reproducibility, indicating a high degree of reversibility of the multi-step reaction. The charge/discharge voltage profiles of these Li-S cells at a current rate of 0.3 C are shown in Figure 3b. The cells had typical sulfur cathode behavior with two discharge potential plateaus at 2.3 and 2.1 V, and two charge potential plateaus at 2.3 and 2.4 V. The length ratios between the upper and lower plateaus were nearly identical for all of the cycles, indicating a high efficiency of sulfur utilization in the SPANI cathode. The discharge capacity value of the cell at the first cycle was  $\sim 937 \text{ mA h g}^{-1}$ , corresponding to a high sulfur utilization of  $\sim 58.2\%$ . However, a large capacity drop between the 1st and the 2nd cycles was observed, which was attributed to the catalytic reduction of electrolyte solvents on the fresh surfaces of SPANI, and the formation of solid electrolyte interface films on the Li-anode in the first cycle (Figure S3).

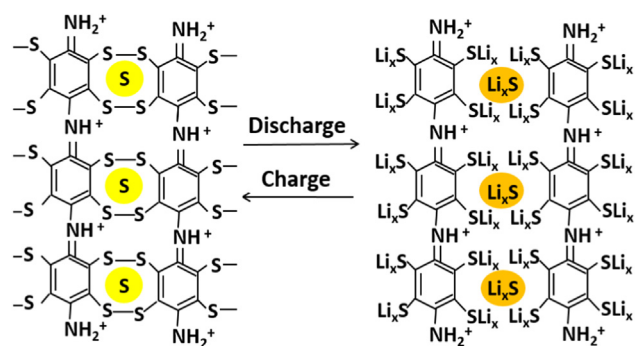
Figure 3c and 3d compared the long-term cycling behavior and Coulombic efficiency of Li-S cells at different discharge/charge current rates. High cycling stabilities were observed at all rates. For example, at 0.3 C, the cell delivered a stable reversible capacity of  $734 \text{ mA h g}^{-1}$  over

200 cycles with a low decay rate (0.051% per cycle). Meanwhile, the cell always had a high Coulombic efficiency of 99.3%, indicating that the poly-shuttle effects were significantly reduced in the cells. Similar cycling performance enhancements were observed at 0.6 and 1 C, over 200 cycles, strongly suggesting that the developed SPANI cathode played a key role in extending the cycling life of Li-S batteries. Even at a high current of 2 C, the cell retained a capacity of above  $700 \text{ mA h g}^{-1}$  after 100 cycles, demonstrating exceptional rate performance. At 2 C, it appeared that the active material took about 100 cycles to reach a steady state in the cathode region to offer stable electrochemical performance because of the solubility of the intermediate lithium polysulfides in the electrolyte, indicating strong affinity of the discharged lithium polysulfides in the SPANI framework [33]. Surprisingly, the Coulombic efficiency of SPANI was consistently decreased with increasing current rates from 0.3 C to 2 C, which was different with the traditional Li-S batteries.

## Discussion

When sulfur covalently bonded on PANI chains, it is not soluble in organic electrolytes during the cell operations, and thus can improve the long-cycle stability of Li-S batteries. However, the capacities of these active sulfur materials decrease. To verify the contribution of disulfide on SPANI, we designed two control experiments based on S and PANI composites. The first one (S/PANI) was fabricated

by simply mixing sulfur and PANI together, and the second one (S-PANI) was fabricated with a traditional heating strategy at 159 °C for 8 h, and then at 280 °C for 2 h in vacuum oven. Both cathodes employing these composites have the same sulfur content with SPANI cathode. The electrochemical performance for both cathodes is shown in Figure S4. As can be seen, at 0.6 C, both electrodes showed inferior cycling stability with a much lower capacity in comparison with SPANI electrode. Of note, the battery had a higher capacity at 2 C than that at 0.6 C and 1 C. The exact mechanisms controlling this unusual phenomenon are still under investigation. One possible explanation is that carbon sulfur bonds (C-S) and disulfide bonds (S-S) on PANI



**Scheme 2** Proposed electrochemical performance of SPANI composites.

chains have different electrochemical performance with elemental sulfur [34]. The proposed mechanism of the SPANI composite is shown in Scheme 2. The disulfide bonds have electrochemical activity due to the intramolecular electrocatalytic effect of the aniline moiety, as well as the improved recombination efficiency from the confined polymer structure that was interconnected with the S-S bonds. During the discharge process, the side chains of S-S functional groups de-polymerized and combined lithium ions to form lithium polysulfides, while the main chain of PANI was stable. During the charge process, a reversed reaction takes place. Generally, the cleavage of S-S bonds and the recombination efficiency are low, since they need a high energy, which was affected by the steric resistant effect of S-S bonds. However, at a larger discharge and charge current rate, an improved recombination efficiency can be achieved, because the S-S bonds could be separated easier. It was confirmed by the larger capacity retention of 700 mA h g<sup>-1</sup> at 2 C than 600 mA h g<sup>-1</sup> at 0.6 C after 200 cycles. This means that the S-S electrochemical cleavage and a recombination process were enhanced at large current rate. Surprisingly, the Coulombic efficiency of Li/SPANI battery was lower at 2 C than that at 0.3, 0.6 and 1 C. The formation and breaking of the S-S bonds may be the key reason for the different Coulombic efficiency change trend, and further work should be performed to research the fundamental reason.

Based on the above analysis, the SPANI cathodes enhanced cycling stability of Li-S batteries. We attributed

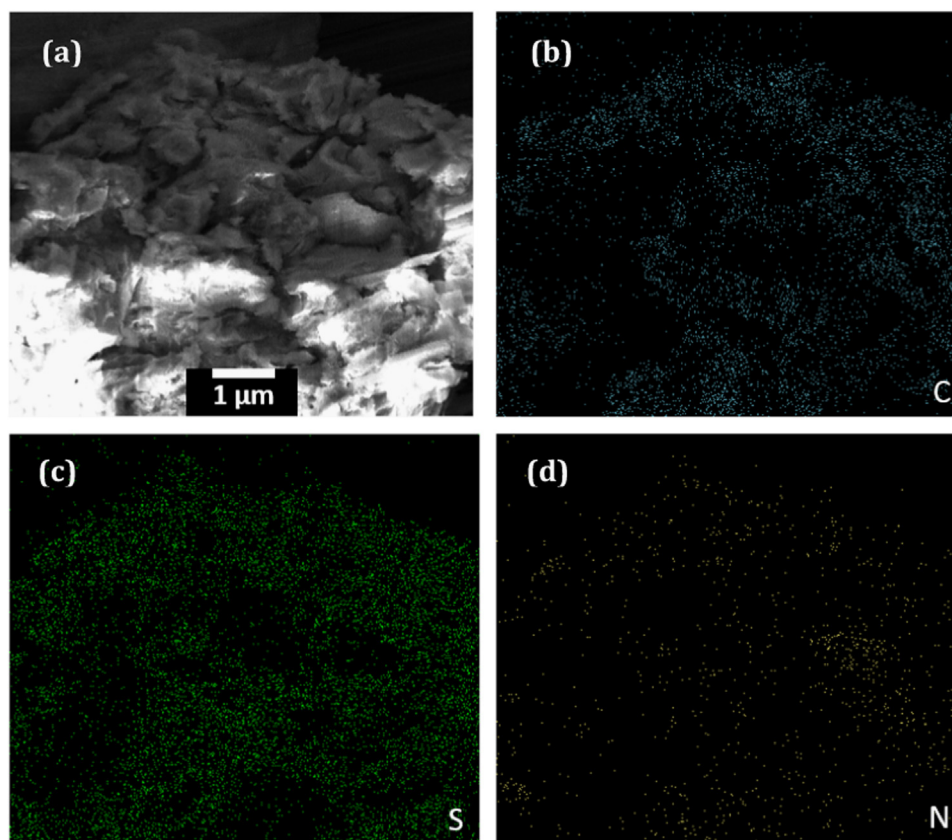


**Figure 4** SEM and EDS mapping data of the cathode after 100 cycles. (a) SEM image of the SPANI cathode after 100 cycles. EDS mapping showing the homogenous distribution of (b) carbon, (c) sulfur, and (d) nitrogen in the SPANI composite, respectively.

the improved performance to the unique structure of SPANI, which not only provided multiple nanopores and strong affinity to trap polysulfide anions during the repeated cycles, but also contained multiple disulfide bonds with electrochemical activity. When comparing the surface morphologies of SPANI with the S-PANI that was fabricated by heating, we observed there were multiple interconnected nanopores on SPANI surface, while the S-PANI had a nanoparticle morphology with a relatively smooth surface without pores (Figure S5). The nanoporous coralloid structure in SPANI was conducive to fast mass transportation within the macrometer size pores, and offered a high degree of interconnectivity of PANI chains to ensure high electron conductivity across the entire structure. In addition, the multiple nano-flakes in the coralloid SPANI structure also accommodated volume change of sulfur and provided large specific surface areas, which not only offered more electroactive sites for sulfur, but also immobilized polysulfides and reduced the aggregation of sulfur. The SEM image of the SPANI cathodes after 100 cycles is shown in Figure 4a. As can be seen, the active sulfur materials were uniformly distributed on the porous coralloid SPANI structure and formed a thick layer, indicating the strong interaction between sulfur and PANI. The corresponding Energy-dispersive X-ray spectroscopy (EDS) mapping was shown in Figure 4b-4d. The density of sulfur materials was much higher than carbon and nitrogen, confirming the existence of both elemental sulfur and disulfide bonds in SPANI materials.

When sulfur was reduced upon fully discharge, the sulfur chemical bonding and a strong interaction between intermediate polysulfides and the SPANI framework was important to hold the active sulfur materials in the cathode and retain effectively electrical contact with the conducting PANI. This assumption was verified by electrochemical impedance spectroscopy spectra (EIS), as shown in Figure S6. When compared with S/PANI composite cathode, the SPANI cathode presented a smaller semicircle at the high-frequency region, since the chemical bonding and strong interactions significantly reduced the charge-transfer resistance in SPANI structure. The improved electronic conductivity together with the enhanced fast mass transportation property might increase the electrocatalytic activity of sulfur toward complete transformation to lithium sulfide ( $\text{Li}_2\text{S}$ ). In addition, the electrostatic interaction between the alkyl ammonium cations and polysulfide anions might also be vital for the effectively entrapment of polysulfides during cycling. As shown in the XPS spectra (Figure S7), the binding energy of N 1s peak was reduced from 399.2 (before cycling) to 398.3 eV (after cycling), indicating the strong interactions of the alkyl ammonium cations with lithium polysulfides.

## Conclusions

In summary, for the first time, we have fabricated nanoporous coralloid SPANI polymers with a two-step chemical process, and showed a bonding stabilization of polysulfides on its long-chain backbones. These covalently bonded polysulfides contributed to high performance of Li-S batteries including high rate capability, long lifespan and high

reversible capacity. The coralloid SPANI structure had triple role in improving electrochemical performance of the SPANI cathodes: (i) it crosslinked to enhance strong contaction between the nonpolar carbon surface and various polar discharge polysulfide species; (ii) it fixed sulfur on SPANI by chemical interaction, and thus reduced the diffusion of polysulfides during cycling; and (iii) it enhanced the electron and ion conductivities in the composite cathode by increasing the meso-pore volumes and surface areas. In addition, the SPANI framework provided a high mechanical stability. Based on this structure, the SPANI demonstrated a superior rate response up to 2 C, and delivered a high performance over 200 cycles with 89.4% capacity retention. The SPANI cathodes may offer a new way to solve the long-term cycling difficulty for sulfur-carbon cathodes and can serve as the basis for significant future work. Further investigations will be conducted to understand the disulfide bond reaction mechanism and enhance the high-rate capability of Li-S cells employing SPANI cathodes.

## Acknowledgments

This work was funded by a Research Challenge Grant (10016089.6.52502) of the West Virginia Higher Education Policy Commission Division of Science and Research. The authors acknowledge use of the WVU Shared Research Facilities and financial support from West Virginia Higher Education Policy Commission Division of Science and Research.

## Appendix A. Supplementary material

Supplementary data associated with this article can be found in the online version at <http://dx.doi.org/10.1016/j.nanoen.2015.10.024>.

## References

- [1] J. Yan, X. Liu, B. Li, *RSC Adv.* 4 (2014) 63268-63284.
- [2] J. Yan, X. Liu, B. Li, *Electrochem. Commun.* 56 (2015) 46-50.
- [3] A. Manthiram, Y. Fu, S. Chung, C. Zu, Y. Su, *Chem. Rev.* 114 (2014) 11751-11787.
- [4] S.S. Zhang, *J. Power Sources* 231 (2013) 153-162.
- [5] G. Zheng, Q. Zhang, J.J. Cha, Y. Yang, W. Li, Z. She, Y. Cui, *Nano Lett.* 13 (2013) 1265-1270.
- [6] G. Zhou, L. Li, C. Ma, S. Wang, Y. Shi, N. Koratkar, W. Ren, F. Li, H. Cheng, *Nano Energy* 11 (2015) 356-365.
- [7] J. Yan, X. Liu, M. Yao, X. Wang, K.T. Wafle, B. Li, *Chem. Mater.* 27 (2015) 5080-5087.
- [8] J. Yan, X. Liu, H. Qi, W. Li, Y. Zhou, M. Yao, B. Li, *Chem. Mater.* 27 (2015) 6394-6401.
- [9] H. Li, X. Yang, X. Wang, M. Liu, F. Ye, J. Wang, Y. Qiu, W. Li, Y. Zhang, *Nano Energy* 12 (2015) 468-475.
- [10] F. Wu, J. Qian, R. Chen, T. Zhao, R. Xu, Y. Ye, W. Li, L. Li, J. Lu, K. Amine, *Nano Energy* 12 (2015) 742-749.
- [11] L. Suo, Y. Zhu, F. Han, T. Gao, C. Luo, X. Fan, Y. Hu, C. Wang, *Nano Energy* 13 (2015) 467-473.
- [12] J. Song, Z. Yu, T. Xu, S. Chen, H. Sohn, M. Regula, D. Wang, *J. Mater. Chem. A* 2 (2014) 8623-8627.
- [13] J. Song, T. Xu, M.L. Gordin, P. Zhu, D. Lv, Y.B. Jiang, Y. Chen, Y. Duan, D. Wang, *Adv. Funct. Mater.* 24 (2014) 1243-1250.
- [14] J. Yan, X. Liu, B. Li, *J. Mater. Chem. A* 3 (2015) 10127-10133.

- [15] S.S. Zhang, *Front. Energy Res.* 1 (2013) 10.
- [16] S. Xin, L. Gu, N.H. Zhao, Y.X. Yin, L.J. Zhou, Y.G. Guo, L. J. Wan, *J. Am. Chem. Soc.* 134 (2012) 18510-18513.
- [17] J. Fanous, M. Wegner, M.S. Spera, M.R. Buchmeiser, *J. Electrochem. Soc.* 160 (2013) A1169-A1170.
- [18] J. Fanous, M. Wegner, J. Grimminger, A. Andresen, M. R. Buchmeiser, *Chem. Mater.* 23 (2011) 5024-5028.
- [19] L. Xiao, Y. Cao, J. Xiao, B. Schwenzler, M.H. Engelhard, L. Saraf, Z. Nie, G.J. Exarhos, J. Liu, *Adv. Mater.* 24 (2012) 1176-1181.
- [20] W. Zhou, Y. Yu, H. Chen, F.J. Disalvo, H.D. Abruña, *J. Am. Chem. Soc.* 135 (2013) 16736-16743.
- [21] S. Zhang, L. Zhang, W. Wang, W. Xue, *Synth. Met.* 160 (2010) 2041-2044.
- [22] D. Li, J. Huang, R.B. Kaner, *Acc. Chem. Res.* 42 (2009) 135-145.
- [23] C.M. Gordana, *Synth. Met.* 177 (2013) 1-47.
- [24] B. Dufour, P. Rannou, D. Djurado, H. Janeczek, M. Zagorska, A. Geyer, J. Travers, A. Pron, *Chem. Mater.* 15 (2003) 1587-1592.
- [25] J. Chiang, A.G. MacDiarmid, *Synth. Met.* 13 (1986) 193-205.
- [26] S.S. Zhang, *Energies* 7 (2014) 4588-4600.
- [27] L. Shi, R. Liang, J. Qiu, *J. Mater. Chem.* 22 (2012) 17196-17203.
- [28] H.Y. Lee, W. Vogel, P.P. Chu, *Langmuir* 27 (2011) 14654-14661.
- [29] X. Yu, J. Xie, J. Yang, H. Huang, K. Wang, Z.S. Wen, *J. Electroanal. Chem.* 573 (2004) 121-128.
- [30] B.J. Kim, S.G. Oh, M.G. Han, S.S. Im, *Langmuir* 16 (2000) 5841-5845.
- [31] C. Beard, P. Spellane, *Chem. Mater.* 9 (1997) 1949-1953.
- [32] J. Zhang, L. Kong, B. Wang, Y. Luo, L. Kang, *Synth. Met.* 159 (2009) 260-266.
- [33] Y. Su, A. Manthiram, *Nat. Commun.* 3 (2012) 1166.
- [34] K. Naoi, K. Kawase, M. Mori, M. Komiyama, *J. Electrochem. Soc.* 144 (1997) L173-L175.



Jianhua Yan is a PhD student in the Department of Mechanical and Aerospace Engineering at West Virginia University from January of 2013. He received his M.S degree in Electronics Engineering from Institute of Microelectronics, Chinese Academy of Sciences in July of 2012. Under the supervision of Profs Xingbo Liu and Bingyun Li, his research focuses on the development of nanostructured materials and renewable materials for energy applications.



Dr. Bingyun Li received his PhD from the Chinese Academy of Sciences in 2000. Currently, he is an Associate Professor with tenure at West Virginia University. Dr. Li is a reviewer for more than 50 journals and an editorial member for more than 10 journals. Dr. Li has authored more than 50 peer-reviewed research articles. He is a member of American Chemical Society, American Society for Microbiology, Materials Research Society, Orthopedic Research Society, and Society for Biomaterials. Dr. Li has given more than 30 invited talks and received awards and prizes from national and international communities.



Xingbo Liu is a Professor and associate Chair for research in the Department of Mechanical and Aerospace Engineering at West Virginia University (WVU). His research interest is primarily concerned with advanced materials for energy storage and conversion. He received his B.S. (1992), M. S. (1995) and Ph.D. (1999) degrees in Materials Science at University of Science and Technology Beijing. Thereafter, he has been involved in the particular fields of solid oxide fuel cell and lithium-type batteries at WVU.